

ond, the short-time dynamics of all the simple fluids over remarkably large ranges of density and temperature are quantitatively described by Eq. (1) which should serve as an important benchmark for theories of the dynamics of dense fluids. Third, the phenomenon of melting has a negligible effect on the short-time dynamics—in marked contrast to the large discontinuities it causes in static properties. Fourth, the measured scattering efficiencies have confirmed recent theoretical estimates for the solid and provide insight into the mechanisms of nonlinear optical effects in simple condensed media.

We are grateful to Dr. N. R. Werthamer for helpful discussions.

¹See, for example, J. R. Hardy and A. M. Karo, in *Light Scattering Spectra of Solids*, edited by G. B. Wright (Springer, New York, 1969), p. 99; M. Krauzman, *ibid.*, p. 109.

²J. P. McTague, P. A. Fleury, and D. B. DuPre, *Phys. Rev.* **188**, 303 (1969); W. S. Gornall, H. E. Howard-Lock, and B. P. Stoicheff, *Phys. Rev. A* **2**, 1288 (1970); J. A. Bucaro and T. A. Litovitz, *J. Chem. Phys.* **55**, 3585 (1971).

³E. Helfand and S. A. Rice, *J. Chem. Phys.* **32**, 1642 (1960).

⁴N. R. Werthamer, R. L. Gray, and T. R. Koehler, *Phys. Rev. B* **2**, 4199 (1970).

⁵We thank D. Batchelder and R. O. Simmons for helpful advice on the care of rare-gas solids.

⁶Y. Kato and H. Takuma, *J. Opt. Soc. Amer.* **61**, 347 (1971).

⁷P. A. Fleury, J. M. Worlock, and W. B. Daniels, *Phys. Rev. Lett.* **27**, 1493 (1971).

⁸R. E. Slusher and C. M. Surko, *Phys. Rev. Lett.* **27**, 1699 (1971).

⁹N. R. Werthamer, private communication; Werthamer, Gray, and Koehler, Ref. 4.

¹⁰R. W. Hellwarth, *J. Chem. Phys.* **52**, 2128 (1970), and references cited therein; R. W. Hellwarth, A. Owyong, and N. George, *Phys. Rev. A* **4**, 2342 (1971).

¹¹J. P. McTague, C. H. Lin, T. K. Gustafson, and R. Y. Chiao, *Phys. Lett.* **32A**, 82 (1970).

Harmonic Generation and Parametric Excitation of Waves in a Laser-Created Plasma

J. L. Bobin, M. Decroisette, B. Meyer, and Y. Vitel

Commissariat à l'Energie Atomique, Centre d'Etudes de Limeil, 94-Villeneuve-Saint-Georges, France

(Received 30 January 1973)

We observed the light emitted along a direction 45° from the beam axis when a Nd-glass laser (frequency ω_0) was focused on a solid target. Quite intense lines were found with frequencies $2\omega_0$, $\frac{3}{2}\omega_0$, $\frac{1}{2}\omega_0$. The lines at $2\omega_0$ and $\frac{3}{2}\omega_0$ are broadened on the low-frequency side only. Their occurrence and broadening may be related to parametric excitation of waves.

Parametric excitation of ion acoustic and Langmuir waves, already observed with microwaves,^{1,2} has been suspected to play an important role in the high-flux interaction of laser light with matter.³ On the other hand, harmonic generation in a plasma has been evidenced either with microwaves in the presence of a magnetic field^{4,5} or with laser light.⁶ The former effect was due to the vicinity of a hybrid resonance whereas the latter was attributed to nonlinear electron conduction.⁷

Observation of the coupling between the two mechanisms will be reported here, the driving frequency being in the optical range.

The experimental arrangement is sketched in Fig. 1. It was partially described in another paper.⁸ Spectral observations were made using a Czerny-Turner grating spectrometer with a mean

dispersion of $8 \text{ \AA}/\text{mm}$ in the first order. For recording in the visible range we used a multichan-

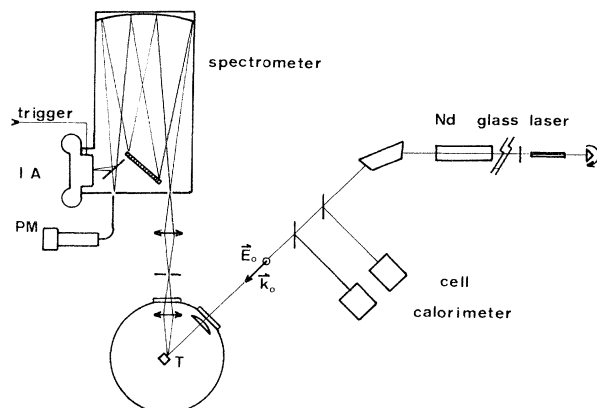


FIG. 1. Experimental setup.

neutron image amplifier (IA) fitted with an S 20 photocathode. Its maximum gain is 10^3 . For wavelengths greater than $1 \mu\text{m}$, we use a 50 CVP photomultiplier tube (PM) connected to the spectrometer by an optical fiber. By means of an appropriate triggering the image amplifier was synchronized with the laser pulse and operated during 50 nsec. The solid hydrogen target is a stick with a square ($1 \text{ mm} \times 1 \text{ mm}$) cross section. The laser pulse generated in a rotating-prism oscillator is tailored by an additional Pockels cell. Amplification through a five-rod cascade provides pulses with a 1-GW peak power, a 15-nsec half-width, and a leading edge shorter than 5 nsec. The focusing lens is plane aspheric: $f = 50 \text{ mm}$ and angular aperture $f/1$. Under these conditions, electron densities of 10^{20} – 10^{21} cm^{-3} and temperatures of a few hundred electron volts

are reached during the leading edge of the pulse.⁹ They prevail for at least the following 5 nsec as indicated by oscillograms of the reflected light.

It is expected that the density gradient, which always exists in such a plasma, plays a major role in harmonic or subharmonic¹⁰ generation. In order to determine the transverse waves which might be subsequently excited, we use the cold-plasma equations. This approximation is valid since in all laboratory experiments for the ω 's and k 's involved, the thermal velocity v_{th} of the electrons is such that $\vec{k} \cdot \vec{v}_{\text{th}} \ll \omega$. Furthermore, we will restrict ourselves to a small region close to a given point r_0 , $|\vec{r} - \vec{r}_0|$ always smaller than the electron excursion in the applied field. Then, expanding with respect to the formal small parameter ϵ which we eventually set equal to 1, the electron velocity and the density of the inhomogeneous plasma are ($e/m\omega_0 = \alpha$)

$$\vec{v}_0 = \vec{v}_0^{(0)} + \vec{v}_0^{(1)} + \vec{v}_0^{(2)} = -\alpha \vec{E}_0 \sin(\omega_0 t - \vec{k}_0 \cdot \vec{r}) - \epsilon(\alpha^2/4c)(\vec{E}_0 \times \vec{B}_0) \cos(2\omega_0 t - 2\vec{k}_0 \cdot \vec{r}) + \epsilon^2(\alpha^3/24c^2)(\vec{E}_0 \times \vec{B}_0) \times \vec{B}_0 \sin(3\omega_0 t - 3\vec{k}_0 \cdot \vec{r}), \quad (1)$$

$$n_0 = N_0 \{1 - (\alpha/\omega_0) \vec{\eta} \cdot \vec{E}_0 \cos(\omega_0 t - \vec{k}_0 \cdot \vec{r}) - \epsilon(\alpha^2/8\omega_0 c) \vec{\eta} \cdot (\vec{E}_0 \times \vec{B}_0) \sin(2\omega_0 t - 2\vec{k}_0 \cdot \vec{r}) + \epsilon^2 \vec{\eta} [\vec{r} - (\alpha^3/72c^2\omega_0)(\vec{E}_0 \times \vec{B}_0) \times \vec{B}_0 \cos(3\omega_0 t - 3\vec{k}_0 \cdot \vec{r})]\}, \quad (2)$$

where E_0 and \vec{k}_0 are the amplitude and wave vector of the applied field, respectively, N_0 is the unperturbed ion density, and $\vec{\eta} = N_0^{-1} \nabla n|_{r=r_0}$ is the density gradient at \vec{r}_0 . In the expansion of v_0 the term in $2\omega_0$ is of the order v/c . However, since in our experiment $\vec{\eta}$ is almost perpendicular to E_0 , one may safely assign the same order of magnitude to the terms in ω_0 and $2\omega_0$ in the expansion of n_0 .

The cold-plasma equations are the same as in the work of Montgomery¹¹ and solved by means of the multiple time-scale expansion,^{12,13}

$$\partial/\partial t \Rightarrow \partial/\partial t + \epsilon \partial/\partial t_1 + \dots, \quad t_1 = \epsilon t \dots$$

The first term on the right-hand side of (1) is of course the zeroth-order solution. The higher-order solutions will include $\vec{v}_0^{(1)}$ and $\vec{v}_0^{(2)}$ which should be simply added to the velocities given below. If we perform a space and time Fourier transform (denoted by a hat), the first-order equation for E is obtained in the form $D\hat{E}_1 = 0$ and the condition $D(\omega_1, \vec{k}_1) = 0$ yields the dispersion relation. Since in our experiment one has $v_0 < v_{\text{th}}$, $\vec{k} \cdot \vec{v}_0$ has been neglected throughout the calculation. If we disregard henceforth the longitudinal part, the first-order solution is ($\alpha_1 = e/m\omega_1$)

$$E_1 = 2\text{Re} \{A_1 \exp[i(\omega_1 t - \vec{k}_1 \cdot \vec{r})] + B_1 \exp[i(\omega_1 t + \vec{k}_1 \cdot \vec{r})]\}, \quad (3)$$

$$v_1 = 2i\alpha_1 \text{Im} \{A_1 \exp[i(\omega_1 t - \vec{k}_1 \cdot \vec{r})] + B_1 \exp[i(\omega_1 t + \vec{k}_1 \cdot \vec{r})]\},$$

where A_1 and B_1 are functions of t_1 which we determine by going to second order. The Fourier transform of the second-order equation for E is

$$D\hat{E}_2 + \hat{S}. \quad (4)$$

Now, we are interested in frequencies close to ω_p . It is well known that if E_0 is high enough, parametric excitation of ion acoustic and Langmuir waves will occur.^{14,15} The ion density oscillates with frequency Ω_s and the electron density with frequency $\omega_L = \omega_0 - \Omega_s$. Then we may replace N_0 by the phenomenological expression

$$N_0 [1 + \eta_s(\Omega_s) + \eta_L(\omega_0 - \Omega_s)],$$

where η_s and η_L are periodical perturbations of zeroth order with respect to the expansions in $\vec{\eta}$ or ϵ . If we keep only the terms leading to lowest order harmonic and subharmonic generation,

$$S = \int dt d^3k \exp[i(\vec{k} \cdot \vec{r} - \omega t)] \{ A(\omega, \omega_1, \vec{k}, \vec{k}_1) + i(\alpha/8c\omega_0^2)\omega_p^2 \vec{\eta} \cdot (\vec{E}_0 \times \vec{B}_0)(1 + \eta_L + \eta_s) \sin(2\omega_0 t - 2\vec{k}_0 \cdot \vec{r}) \vec{v}_1 \\ - 4\pi e N_0 \vec{\eta} \cdot [\vec{r} - (\alpha^3/72c^2\omega_0)(\vec{E}_0 \times \vec{B}_0) \times \vec{B}] \cos(3\omega_0 t - 3\vec{k}_0 \cdot \vec{r})(1 + \eta_L + \eta_s) \vec{v}_0^{(0)} + \dots \}, \quad (5)$$

The right-hand side of (5) leads to δ functions of frequency and wave-vector combinations:

$$\delta(\omega - \omega_1) \delta(\vec{k} - \vec{k}_1), \quad (6)$$

$$\delta(\omega - 3\omega_0 + \Omega_s + \omega_1) \delta(\vec{k} - 2\vec{k}_0 - \vec{k}_L + \vec{k}_1), \quad \delta(\omega - 2\omega_0 \pm \Omega_s) \delta(k - 2k_0 \pm k_s), \quad (7)$$

$$\delta(\omega - \omega_0 - \Omega_s + \omega_1) \delta(\vec{k} - \vec{k}_0 + \vec{k}_L + \vec{k}_1).$$

Possible modes (ω_1, \vec{k}_1) make D vanish. Therefore, the coefficient of the corresponding term in the right-hand side of (5) should also vanish in order to get a finite solution for (4). Associating (6) with the first element of the set (7) one should have

$$\omega_1 = \frac{1}{2}(3\omega_0 - \Omega_s), \quad 2\vec{k}(\frac{3}{2}\omega_0 - \frac{1}{2}\Omega_s) = 2\vec{k}_0 + \vec{k}_L, \quad (8)$$

and the condition on the coefficient gives

$$A_1 = a_1 \exp(\gamma_1 t_1) + a_1' \exp(-\gamma_1 t_1) \quad (9)$$

with growth rate

$$\gamma_1 = (\alpha/16c\omega_0^2)\omega_p^2 \vec{\eta} \cdot (\vec{E}_0 \times \vec{B}_0) \mathcal{E}_L, \quad (10)$$

\mathcal{E}_L being the amplitude of the perturbation due to the Langmuir wave. By the same token one may have more growing modes such as

$$\omega_1 = 2\omega_0 \pm \Omega_s, \quad \vec{k}(2\omega_0 \pm \Omega_s) = 2\vec{k}_0 \pm \vec{k}_s, \quad (11)$$

$$\omega_1 = \frac{1}{2}(\omega_0 + \Omega_s), \quad 2\vec{k}(\frac{1}{2}\omega_0 + \frac{1}{2}\Omega_s) = \vec{k}_0 + \vec{k}_L. \quad (12)$$

Since $\vec{k}_0 = \vec{k}_L + \vec{k}_s$, by virtue of a dispersion relation of the usual plasma type, one cannot have $2\vec{k}(\frac{3}{2}\omega_0 - \frac{1}{2}\Omega_s) = \vec{k}(2\omega_0 + \Omega_s)$. Thus, in the case (11), only the wave $(2\omega_0 - \Omega_s, 2\vec{k}_0 - \vec{k}_s)$ is allowed. The wave near $\frac{1}{2}\omega_0$ cannot be excited at points where $\omega_p = \omega_0$, but at lower densities where little effect of parametrically excited longitudinal waves is expected.

Now, lines are actually observed with frequencies around $2\omega_0$, $\frac{3}{2}\omega_0$, and $\frac{1}{2}\omega_0$. These lines build up during the leading edge of the laser pulse, reach their maximum at the incident peak power, and afterwards decay faster than the incoming light. The accuracy of the time measurements is 2 nsec. Each time-integrated spectral profile of the lines at $2\omega_0$ and $\frac{3}{2}\omega_0$ is recorded in a single shot with the image amplifier, whereas the line at $\frac{1}{2}\omega_0$ needs several shots to be recorded with the photomultiplier. The profiles are plotted in Fig. 2. The incident radiation is composed of about 45 lines spaced 0.95 Å apart. The envelope is nearly symmetrical with 30 Å half-width.

None of the observed lines are polarized. Profiles of lines at $2\omega_0$ and $\frac{3}{2}\omega_0$ are asymmetric and broadened towards lower frequencies only. The

width of the broadened part is almost the same on the wavelength scale. This gives a $\Delta\omega$ twice as large at $2\omega_0$ as at $\frac{3}{2}\omega_0$, in agreement with (8) and (11). It was checked that the broadening cannot be explained by a Doppler shift due to the gas dynamic motion of the laser-created plasma. The intensity at $\frac{3}{2}\omega_0$ is larger than at $2\omega_0$. This might come from the direction of the density gradient, which is roughly parallel to the laser-beam axis.

The present experiment shows that harmonic

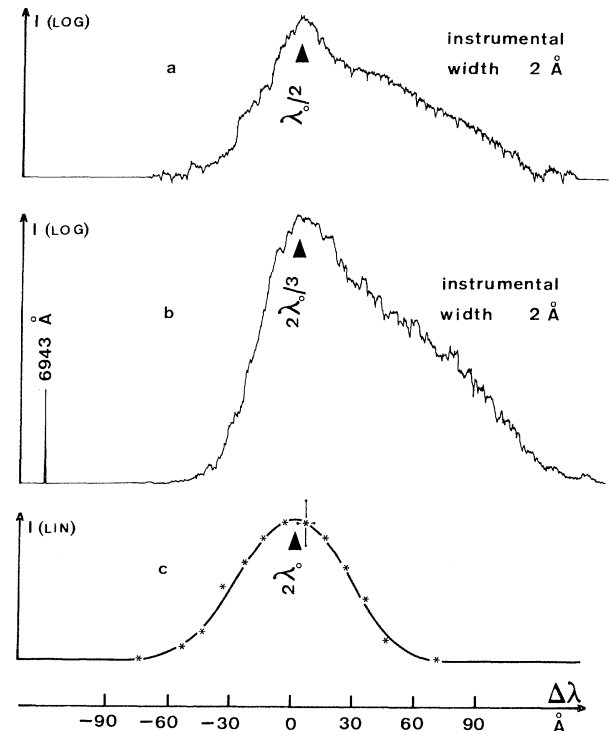


FIG. 2. Spectral profile of the three observed harmonics plotted versus the wavelength shift from the central wavelength. (a) $2\omega_0$ harmonic; (b) $\frac{3}{2}\omega_0$ harmonic; (c) $\frac{1}{2}\omega_0$ harmonic. Vertical scales are arbitrary.

generation and line broadening may depend on both the density gradient and the parametric excitation of longitudinal waves. The high-frequency part of the spectrum of ion acoustic waves is thus directly visible. Detailed temporal behavior of the harmonic lines is under investigation.

The authors are indebted to J. L. Bocher, J. F. Mengue, and G. Pantigny for technical assistance.

¹K. Kato, M. Yoseli, S. Kiyama, and S. Watanabe, *J. Phys. Soc. Jap.* **20**, 2097 (1965).

²R. A. Stern and N. Tzoar, *Phys. Rev. Lett.* **17**, 903 (1966).

³M. Waki, T. Yamanaka, H. B. Kang, K. Yoshida, and C. Yamanaka, *Jap. J. Appl. Phys.* **11**, 420 (1972).

⁴R. Cano, I. Fidone, M. J. Schwartz, and B. Zanfagna, in *Proceedings of the International Conference*

on Phenomena in Ionized Gases, Oxford, England, 1971 (to be published).

⁵S. L. Tetenbaum, R. F. Whitmer, and E. B. Barrett, *Phys. Rev.* **135**, A374 (1964).

⁶M. Decroisette, B. Meyer, and G. Piar, *J. Phys. C: Proc. Phys. Soc., London* **32**, 56, 119 (1971).

⁷R. Jancel, *Nuovo Cimento, Suppl.* **6**, 1329 (1968).

⁸M. Decroisette, J. Peyraud, and G. Piar, *Phys. Rev. A* **5**, 1391 (1972).

⁹J. L. Bobin, F. Delobbeau, G. de Biouvanni, C. Fauquignon, and F. Floux, *Nucl. Fusion* **9**, 115 (1969).

¹⁰C. S. Chen, *J. Plasma Phys.* **5**, 107 (1971).

¹¹D. Montgomery, *Physica (Utrecht)* **31**, 693 (1965).

¹²E. A. Frieman, *J. Math. Phys. (N.Y.)* **4**, 410 (1963).

¹³G. Sandri, *Ann. Phys. (New York)* **24**, 332 (1963).

¹⁴V. P. Silin, *Zh. Eksp. Teor. Fiz.* **48**, 1679 (1965) [*Sov. Phys. JETP* **21**, 1127 (1965)].

¹⁵K. Nishikawa, *J. Phys. Soc. Jap.* **24**, 916, 1152 (1968).

Refraction by the Electromagnetic Pump of Parametrically Generated Electrostatic Waves*

Donald Arnush and Charles F. Kennel†
TRW Systems, Los Angeles, California 90278
 (Received 22 May 1972)

In certain ionospheric and laboratory parametric-decay-instability experiments, pump-dependent refraction modifies the nature of the instabilities. In the ionosphere, electrostatic waves can be trapped in the gradients of the high-frequency pump. In the laboratory the refraction, and hence the convective nature of the instability, is determined completely by the pump. These simple examples suggest that pump-energy absorption may be enhanced by tailoring the pump profile to create a nonconvective instability.

Parametric plasma-wave generation by electromagnetic waves frequency-matched to the electron plasma frequency has been detected from microwave irradiation of the *F* region of the ionosphere,^{1,2} and plays a major role in laser-pellet interactions. One feature common to all three configurations is a plasma density gradient, which localizes the parametric amplification region. Perkins and Flick³ argue that propagation out of the pump-plasma wave of the frequency-matching region limits wave amplification and pump energy absorption. They consider only the influence of plasma gradients upon wave propagation. However, in the frequency-matching region, the real part of the plasma wave frequency, as well as its imaginary part, depends upon pump amplitude. Then, since pump gradients are much stronger than plasma gradients, a small-amplitude pump may modify wave propagation. We discuss two examples of pump-dependent refraction. For a pump matched to the peak *F*-region iono-

spheric plasma frequency, the local plasma density gradients are weak, and the pump amplitude oscillates many times within the amplification region. A pump near instability threshold can "trap" electrostatic waves in its gradients, and so induce a nonconvective instability. In laboratory plasmas ($T_e/T_i \gg 1$) the parametrically generated modes have an ion-acoustic nature, whose refraction is due only to the pump, when T_e is uniform. Here the spatial gradients of the pump amplitude matter less than those of the resonant coupling to the pump. Most unstable modes are weakly convective, but some can be trapped at appropriate locations within the resonant-coupling region.

We will consider one-dimensional plasmas with density gradients, pump propagation, and pump-power variations along *z* only, with the pump electric field E_0 , of frequency ω_0 , polarized in the *y* direction of a Cartesian coordinate system. The Hamiltonian equations of motion of a wave